

Deep EEG Super-resolution: Upsampling EEG Spatial Resolution with Generative Adversarial Networks

Isaac A. Corley, Member, IEEE, Yufei Huang, Senior Member, IEEE

Abstract— Electroencephalography (EEG) activity contains a wealth of information about what is happening within the human brain. Recording more of this data has the potential to unlock endless future applications. However, the cost of EEG hardware is increasingly expensive based upon the number of EEG channels being recorded simultaneously. We combat this problem in this paper by proposing a novel deep EEG super-resolution (SR) approach based on Generative Adversarial Networks (GANs). This approach can produce high spatial resolution EEG data from low resolution samples, by generating channel-wise upsampled data to effectively interpolate numerous missing channels, thus reducing the need for expensive EEG equipment. We tested the performance using an EEG dataset from a mental imagery task. Our proposed GAN model provided $\sim 10^4$ fold and $\sim 10^2$ fold reduction in mean-squared error (MSE) and mean-absolute error (MAE), respectively, over the baseline bicubic interpolation method. We further validate our method by training a classifier on the original classification task, which displayed minimal loss in accuracy while using the super-resolved data. The proposed SR EEG by GAN is a promising approach to improve the spatial resolution of low density EEG headset.

I. INTRODUCTION

Electroencephalography (EEG) is a noninvasive neuroimaging modality widely used for clinical diagnosis of seizures and cognitive neuroscience. It has gained increasing popularity in recent years as a neurofeedback device in brain-computer interface (BCI) systems with applications including typing interface for locked-in patients, neurorehabilitation [1], brain-controlled drone [2], and detection of driver fatigue [3]. However, a primary bottleneck to EEG-based BCI research is the cost of hardware. Ideally, EEG devices with high density channels are preferred in order to obtain recordings of brain activities with high spatial resolution underlying different cognitive events. However, the cost of EEG hardware increases exponentially with channels, with a majority of commercial EEG devices with 32 channels costing more than \$20k. For academia and industry, this can greatly hinder the quality of products and research being performed. This also results in poor generality for EEG-based algorithms because prediction algorithms developed using one headset cannot be used for a headset of different channels even if both are used to measure the same cognitive events. EEG channel interpolation has been proposed in many research efforts [4][5] to recreate missing

or defective sensor channels. Although they showed favorable improvement for single selective channel interpolation, research for interpolating many channels at a global scale is scarce.

Deep learning and its applications have recently become highly popular and rightly so, due to their superior ability to learn representations of complex data [6]. One of its applications is image super-resolution (SR), where deep learning based pixel interpolation was developed [7] to generate high resolution (HR) copies from low resolution (LR) images. The state-of-the-art SR performance is obtained by the new game theoretic deep generative model of Generative Adversarial Networks (GANs) [8], which established the first framework to achieve photo-realistic natural images for a 4x upscaling factor [9].

Inspired by the similarity between global EEG channel interpolation and image SR along with the superb image SR performance achieved by GANs, we propose deep EEG super-resolution, a novel framework for generating high spatial resolution EEG data from low resolution recordings using GANs. We compare our work to a baseline of bicubic interpolation and then additionally verify performance through training a classifier using the SR EEG data for the original EEG dataset's classification purpose.

II. DATA

A. Berlin BCI Competition III, Dataset V

Dataset V of the Berlin Brain Computer Interface Competition III provided by the IDIAP Research Institute [10] was used. The dataset consists of 32 EEG channels recorded at 512 Hz for 3 individual subjects, located at the standard positions of the International 10-20 system (Fp1, AF3, F7, F3, FC1, FC5, T7, C3, CP1, CP5, P7, P3, Pz, PO3, O1, Oz, O2, PO4, P4, P8, CP6, CP2, C4, T8, FC6, FC2, F4, F8, AF4, Fp2, Fz, Cz). The dataset was initially used for a mental imagery multiclass classification competition of three labeled tasks. The data is provided with train and test sets for each subject; however, only the train set was used due to the test set not being provided with labels. The train set contained a total of 1,096,192 samples.

B. Preprocessing

Following the epoch extraction procedure in [10], the raw data was separated into epochs of length 512 samples using a moving window with a stride of 32 samples. This resulted in epochs of size (32 channels by 512 samples). The epoched data was then split into train, validation, and test sets for holdout validation using a 75/20/5 percentage split criterion.

The initial Dataset V classifiers used precomputed features, which consisted of the estimated power spectral

I. A. Corley is an Engineer at Southwest Research Institute (SwRI) and a graduate student of Electrical Engineering at the University of Texas at San Antonio, San Antonio, TX 78249 USA (e-mail: icorley@swri.org).

Y. Huang is with the Department of Electrical and Computer Engineering, University of Texas at San Antonio, San Antonio, TX 78249 USA (e-mail: yufei.huang@utsa.edu).

Deep EEG Super-resolution: Upsampling EEG Spatial Resolution with Generative Adversarial Networks

IsaacA.Corley Ieee会员 YufeiHuang SeniorMember IEEE

摘要：脑电图（EEG）活动包含有关人脑内发生的事情的丰富信息。记录更多这些数据有可能解锁无穷无尽的未来应用程序。然而，基于同时记录的EEG通道的数量，EEG硬件的成本越来越昂贵。在本文中，我们提出了一种基于生成对抗网络（GANs）的新型深脑电超分辨率（SR）方法来解决这个问题。这种方法可以从低分辨率样本中产生高空间分辨率的EEG数据，通过生成

以有效地内插众多缺失的信道，从而减少对昂贵的脑电设备的需要。我们使用心理图像任务的EEG数据集测试了性能。我们提出的GAN模型提供了平均平方误差（MSE）和平均绝对误差的~104倍和~102倍的减少

基线双三次插值法。我们通过在原始分类任务上训练分类器来进一步验证我们的方法，该分类器在使用超解析数据时显示出最小的精度损失。GAN提出的SREEG是提高低密度EEG耳机空间分辨率的有希望的方法。

I. INTRODUCTION

一种广泛用于癫痫发作临床诊断和认知神经科学的无创神经影像学方法。近年来，它作为脑机接口（BCI）系统中的神经反馈设备越来越受欢迎，其应用包括

锁定患者，神经稳定[1]，脑控无人机[2]和驾驶员疲劳检测[3]。然而，基于脑电图的BCI研究的主要瓶颈是硬件成本。理想情况下，具有高密度通道的EEG设备是优选的，以便获得在不同认知事件基础上具有高空间分辨率的大脑活动的记录。然而脑电硬件的成本与渠道成倍增加与大多数商业脑电设备32通道成本超过costing20k。对于学术界和工业界这可以极大地阻碍正在进行的产品和研究的这也导致基于EEG的算法的通用性差，因为使用一个耳机开发的预测算法不能用于不同信道的耳机，即使两者都用于测量相同认知事件。在许多研究工作中已经提出了EEG通道插值[4][5]来重新创建缺失

B. Preprocessing

按照[10]中的历元提取程序，使用步幅为32个样本的移动窗口将原始数据分离为长度为512个样本的历元。这导致了大小的时代（32个通道乘512个样本）。然后，使用75205百分比拆分标准将划时代的数据拆分为列车，验证和测试集，以进行持久验证。

初始数据集V分类器使用了由估计功率谱组成的预算计算特征

或有缺陷的传感器通道。虽然他们表现出有利选择性信道内插，用于在全球范围内插许多信道的研究是稀缺的。

深度学习及其应用最近变得非常流行，这是正确的，因为它们具有学习复杂数据表示的卓越能力[6]。其应用之一是图像超分辨率（SR），其中开发了基于深度学习的像素插值[7]，以从低分辨率（LR）图像生成高分辨率（HR）副本。最先进的SR性能是通过生成对抗网络（GANs）的新博弈论深度生成模型获得的[8]，该模型建立了第一个以4x升尺度因子实现照片逼真自然图像的框架[9]。

基于全局脑电通道插值与图像SR之间的相似性，以及GANs所实现的卓越的图像SR性能，我们提出了一种利用GANs从低分辨率记录中生成高空间分辨率脑电数据的新框架。我们将我们的工作与双三次插值的基线进行比较，然后通过使用SREEG数据训练分类器来验证性能。

II. 数据

A. 柏林BCI竞赛III，数据集V

柏林脑计算机接口的数据集V由IDIP研究所[10]提供的竞赛III被使用该数据集由32个以512Hz记录的EEG通道组成，用于3个个体受试者，位于国际10-20系统的标准位置（Fp1, AF3, F7, F3, FC1, F4, F8, Af4, Fp2, Fz, Cz）。该数据集最初用于三个标记任务的心理图像多类分类竞赛。数据随每个受试者的火车和测试集一起提供；但是，由于测试集没有提供标签，因此只使用了火车集。列车组共包含1 096 192个样本。

I.A.Corley是西南研究所（SwRI）的工程师，也是德克萨斯大学圣安东尼奥分校电气工程研究生，圣安东尼奥，德克萨斯州78249USA（电子邮件：icorley@swri.org）。

Y.Huang在电气和计算机系工作，德克萨斯大学圣安东尼奥，圣安东尼奥，TX78249 USA（电子邮件：yufei.huang@utsa.edu）。

density (PSD) of each epoch in the band 8-30 Hz with a frequency resolution of 2 Hz for the 8 centro-parietal channels (C3, Cz, C4, CP1, CP2, P3, Pz, P4), which resulted in a 96-dimensional vector (8 channels, 12 frequency components).

For use with super-resolution models, all datasets were reshaped to epochs of size (32 channels by 64 samples). To produce the low-resolution (LR) data, the epochs were downsampled by channel based upon the scale factor used, e.g., downsampling 32 channels by a scale factor of 2 would remove every other channel, leaving 16 channels of LR data. The removed channels are then used as the HR data. The input data and its corresponding ground truth were then standard-normalized to a mean $\mu = 0$ and standard deviation $\sigma = 1$ using the mean and standard deviation of the input channel training set. This was repeated using the same statistics for normalizing the validation and test data.

III. METHODS

A. Generative Adversarial Networks

Generative Adversarial Networks (GANs) are an unsupervised deep learning framework recently proposed by Goodfellow et al. [8]. The framework is composed of two networks, a generator G and a discriminator D , optimized to minimize a two-player minimax game, where the generator learns to fool the discriminator and the discriminator learns to prevent itself from being fooled. As Goodfellow et al. [8] describes, "The generative model can be thought of as analogous to a team of counterfeiters, trying to produce fake currency and use it without detection, while the discriminative model is analogous to the police, trying to detect the counterfeit currency." During training of GANs, the generator is fed an input noise vector and produces an output distribution P_G . The discriminator is then trained to learn to discriminate between P_G and the true data distribution, P_{Data} . Additionally, the generator is trained to learn how to further fool the discriminator. Theoretically P_G will converge to P_{Data} with the discriminator being unable to differentiate between generated and true samples, resulting in an ideal generative model which can produce data following the true data distribution.

While GANs are a powerful framework, they possess stability issues which cause the adversarial networks to rarely reach convergence. Variations of the framework, namely Wasserstein GANs (WGANs) [11][12], have been developed which use different loss functions with properties that improve training stability. In contrast to the original GAN framework, WGANs minimize the Earth Mover's Distance (Wasserstein-1 Distance) and attempt to constrain the gradient norm of the discriminator's output with respect to its input using a gradient penalty in the loss function. We adopt the WGAN framework for training throughout our research as we experienced improved stability over the original GAN framework.

B. Proposed Wasserstein Generative Adversarial Networks for EEG Super Resolution

Our proposed WGAN model for EEG SR also consists of a generator and a discriminator. The generator architecture consists of the sequence of layers detailed in Figure 1, with

the parameters detailed in TABLE I. Similarly to [11] we adopt a modified sequence of convolutional layers, which allow EEG data to be processed by Convolutional Neural Networks (CNNs) due to correlations across channels. This sequence is composed of convolutional layers with kernel dimensions that find the relationships between channels, $(n, 1)$, where $n = (\# \text{ input channels} + 1)$. All convolutional layers enforce the same zero-padding to keep the same dimensions throughout. This sequence is then fed into one dense block [14] composed of 3 densely connected convolutional sequences, followed by a convolutional layer whose outputs are the super resolved channels. Note that the upsampling layer and the first subsequent convolutional layer are unique to SR models for a scale factor of 4 as the input channels need to be upsampled by 3 channel-wise.

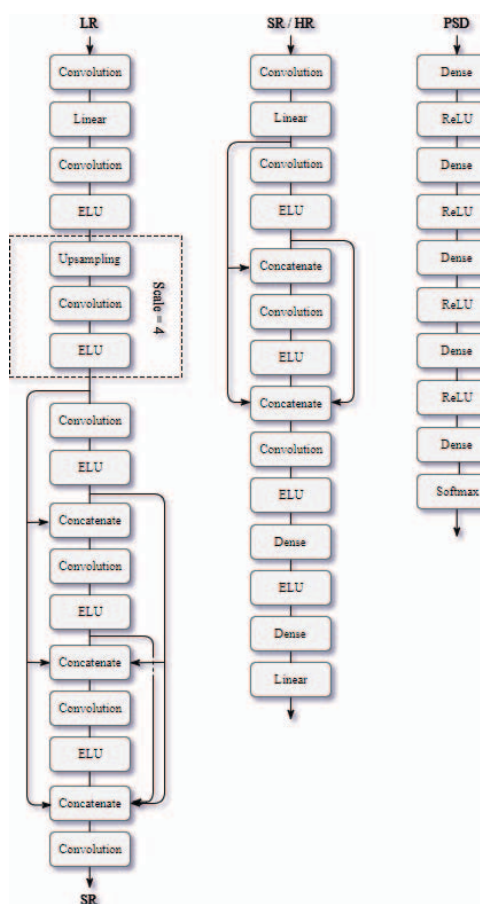


Figure 1. Model Architectures. Generator (left), Discriminator (center), Classifier (right)

TABLE I. GENERATOR MODEL ARCHITECTURE

Layer Type	Kernels	Dimensions	Activation
Convolution	128	(# input channels + 1, 1)	Linear
Convolution	128	(# input channels / 2 + 1, 1)	ELU
Upsampling	-	(scale factor - 1, 1)	-
Convolution	128	(# input channels + 1, 1)	ELU
Convolution	128	(# input channels / 2 + 1, 1)	ELU

8-30赫兹波段中每个周期的密度 (PSD) , 频率分辨率为2赫兹, 用于8个中心顶叶通道 (C3, Cz, C4, CP1, CP2, P3, Pz, P4) , 从而产生96维矢量 (8个通道, 12个频率分量) 。

为了与超分辨率模型一起使用, 所有数据集都被重塑为大小的时代 (32个通道乘64个样本) 。为了产生低分辨率(LR)数据, 根据所使用的比例因子, 逐通道对历年进行下采样, 例如, 以2的比例因子对32个通道进行下采样, 将删除每个其他通道, 留下16然后将删除的通道用作HR数据。然后, 使用输入通道训练集的均值和标准差将输入数据及其相应的基真标准归一化为均值 $\mu=0$ 和标准差 $\sigma=1$ 。这是重复使用相同的统计标准化验证和测试数据。

III. 方法

A.生成对抗网络

生成对抗网络 (GANs) 是Goodfellow等人最近提出的一种无监督的深度学习框架。[8]该框架由两个网络组成, 一个生成器G和一个鉴别器D, 优化以最小化两个玩家minimax游戏, 其中生成器学习愚弄鉴别器, 鉴别器学习防止自己被愚弄。正如Goodfellow等人。[8]描述说: "生成模型可以被认为类似于一群造假者, 试图制造假货币

虽然鉴别模型类似于警察, 试图检测假币。"在GANs的训练期间, 发生器被馈送输入噪声矢量并产生输出分布 P_G 。然后训练鉴别器以学习区分 P_G 和真实数据分布 P 数据。此外, 生成器被训练以学习如何进一步愚弄鉴别器。理论上, P_G 将收敛于 P 数据, 而鉴别器无法区分生成的样本和真实的样本, 从而产生一个理想的生成模型, 该模型可以产生遵循真实数据分布的数据。

虽然甘斯是一个强大的框架, 但它们具有稳定性问题, 导致对抗网络很少达到收敛。已经开发了框架的变体, 即Wasserstein GANs (WGANs) [11][12], 其使用具有提高训练稳定性的属性的不同损失函数。与原始GAN框架相反, WGAN将地球最小化 (Wasserstein-1距离) 并试图约束

在损失函数中使用梯度惩罚的 s 输入。我们在整个研究过程中采用WGAN框架进行培训, 因为我们经历了比原始GAN框架更高的稳定性。

与[11]类似, 我们采用了经过修改的卷积层序列, 由于通道之间的相关性, 卷积神经网络 (CNNs) 可以处理脑电图数据。该序列由具有内核维度的卷积层组成, 这些层查找通道之间的关系, $(n, 1)$, 其中 $n= (\# \text{输入通道} + 1)$ 。所有卷积层都强制执行相同的零填充, 以始终保持相同的尺寸。然后, 这个序列被送入一个由3个密集连接的卷积序列组成的密集块[14], 然后是一个卷积层, 其输出是超分辨率通道。请注意, 上采样层和第一个后续卷积层对于比例因子为4的SR模型是唯一的, 因为输入通道需要按3通道进行上采样。

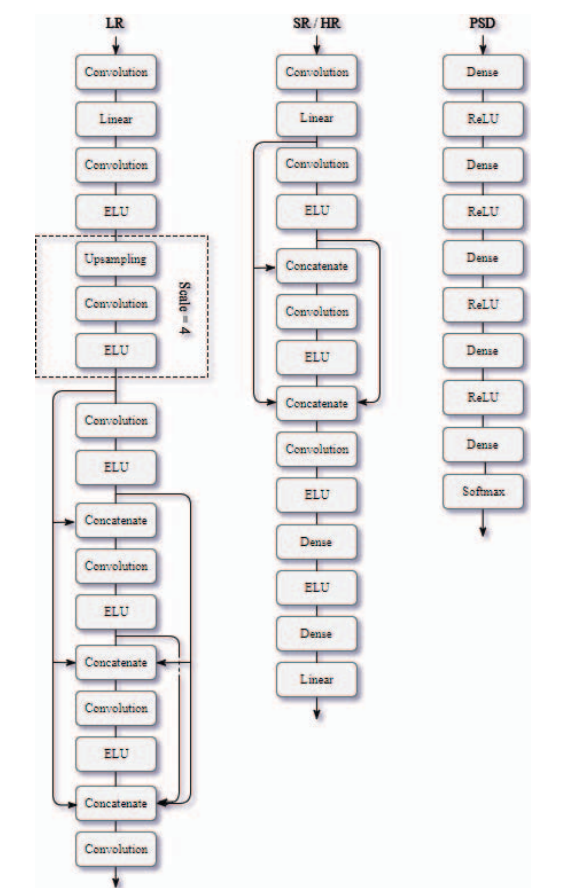


图1。模型架构。生成器 (左) , 鉴别器 (中)
Classifier (right)

TABLE I. GENERATOR MODEL ARCHITECTURE

层类型	Kernels	Dimensions	Activation
Convolution	128	(#输入通道+1, 1)	Linear
Convolution	128	(#输入通道/2+1, 1)	ELU
Upsampling	-	(scale factor - 1, 1)	-
Convolution	128	(#输入通道+1, 1)	ELU
Convolution	128	(#输入通道/2+1, 1)	ELU

B.提出的用于脑电超分辨率的Wasserstein生成对抗网络
我们提出的用于脑电SR的WGAN模型也由生成器和鉴别器组成。生成器架构由图1中详述的层序列组成。与

Layer Type	Kernels	Dimensions	Activation
Concatenate	-	-	-
Convolution	256	(# input channels / 2 + 1, 1)	ELU
Concatenate	-	-	-
Convolution	512	(# input channels / 2 + 1, 3)	ELU
Concatenate	-	-	-
Convolution	1	(# input channels + 1, 1)	None

The discriminator follows a similar scheme to the generator architecture aside from a few key differences detailed in TABLE II. The 4th convolutional layer has a stride of (4, 4) and is fed into a fully-connected layer. The final output activation of the model is linear to comply with the WGAN framework.

As in [9], the generator's parameters are first initialized through training the network in a supervised manner to map the downsampled LR data to the HR counterparts using a mean-squared error (MSE) loss function. This was found to prevent converging to local minima. The generator is then inserted into the GAN training process to fine-tune the model and find more optimal parameters in comparison to only using a distance metric as a loss function.

TABLE II. DISCRIMINATOR MODEL ARCHITECTURE

Layer Type	Kernels	Dimensions	Activation
Convolution	64	(# input channels + 1, 1)	Linear
Convolution	64	(1, 3)	ELU
Concatenate	-	-	-
Convolution	128	(# input channels / 2 + 1, 1)	ELU
Concatenate	-	-	-
Convolution	256	(# input channels / 4 + 1, 3)	ELU
Fully-Connected	128	-	ELU
Fully-Connected	1	-	Linear

IV. RESULTS

A. Training & Hyperparameters

Dropout regularization [15] was applied at the output of every activation within both the generator and discriminator excluding the output layers. The generator and discriminator had dropout rates of 0.1 and 0.25, respectively. The α parameter for all ELU [16] activations was set to 1. The Adam optimizer [17] was used throughout with learning rate $\alpha = 10^{-4}$, $\beta_1 = 0.5$, and $\beta_2 = 0.9$. The generator network was first pre-trained using a MSE (L2) loss for 50 epochs with a mini-batch size of 64. All hyperparameters were tuned to optimize performance on the validation set.

The pre-trained generator was then fine-tuned using the WGAN framework losses using a gradient penalty weight of 10. The GAN training ratio was set to 3, which updates the discriminator once for every 3 generator updates. In addition to the WGAN loss function, a modification was made to

multiply the WGAN loss by a factor of 10^{-2} and add a MSE loss on the generator output. This was inspired by the feature matching procedure from [18], which specifies additional objectives for the generator to prevent from overtraining on the discriminator. Also from [18], the label smoothing technique was incorporated, to assist in avoiding converging to local minima.

An evaluation of the model outputs of the validation and test datasets are displayed in TABLE III. The quantitative results are compared to a baseline of bicubic interpolated channel data. Both MSE and mean absolute error (MAE) between upsampled and true EEG signals were calculated.

TABLE III. SUPER RESOLUTION PERFORMANCE RESULTS

Dataset	Scale	Bicubic		WGAN	
		MSE	MAE	MSE	MAE
Val	2	3.71E7	3.89E3	2.01E3	24.38
	4	7.23E7	6.42E3	8.53E3	63.83
Test	2	3.75E7	3.91E3	2.06E3	24.66
	4	7.30E7	6.45E3	8.68E3	64.39

B. Dataset V Classification Super Resolution Performance

To further evaluate the validity of the SR data, we investigated the performance of classifying the mental imagery classes using the SR data. Deep neural network (DNN) classifiers were trained for both the precomputed features of the HR and SR data using the precomputed feature class labels. The DNN classifier consisted of 5 dense layers with 512, 256, 128, 64, and 3 neurons per layer, respectively. All layers contained ReLU [19] activations excluding the output layer which consisted of a Softmax activation. The classifiers were trained using a categorical cross-entropy loss optimized by the ADAM optimizer with learning rate $\alpha = 10^{-3}$, $\beta_1 = 0.9$, and $\beta_2 = 0.99$. The class predictions with multiple metrics for the DNNs trained using the ground truth HR data and SR data by WGAN are recorded in TABLE IV.

TABLE IV. CLASSIFICATION PERFORMANCE RESULTS

Scale	Metric (%)	Class	HR		WGAN	
			Val	Test	Val	Test
2	Precision	Accuracy	-	89.56	87.75	85.63
		Precision	2	89.70	86.65	83.98
		Precision	3	89.48	87.54	85.80
	Recall	Precision	7	89.57	88.77	86.80
		Recall	2	87.66	84.33	83.86
		Recall	3	88.49	88.57	83.84
		Recall	7	92.06	89.62	88.69
4	Precision	Precision	Accuracy	-	89.56	87.75
		Precision	Precision	2	89.70	86.65
		Precision	Precision	3	89.48	87.54
	Recall	Precision	Precision	7	89.57	88.77
		Recall	Precision	2	87.66	84.33
		Recall	Precision	3	88.49	88.57
		Recall	Precision	7	92.06	89.62

层类型	Kernels	Dimensions	Activation
Concatenate	-	-	-
Convolution	256	(#输入通道2+1 1)	ELU
Concatenate	-	-	-
Convolution	512	(#输入通道2+1 3)	ELU
Concatenate	-	-	-
Convolution	1	(#输入通道+1 1)	None

将WGAN损耗乘以10⁻²的系数，并在发电机输出上加上MSE损耗。这受到[18]的特征匹配程序的启发，该程序为生成器指定了额外的目标，以防止在鉴别器上过度训练。同样从[18]，标签平滑技术被纳入，以帮助避免收敛到局部极小值。

对验证和测试数据集的模型输出的评估显示在表三中。将定量结果与双三次插值通道数据的基线进行比较。计算了上采样和真脑电信号之间的MSE和平均绝对误差(MAE)。

表三。 SUPER RESOLUTION PERFORMANCE RESULTS

Dataset	Scale	Bicubic		WGAN	
		MSE	MAE	MSE	MAE
Val	2	3.71E7	3.89E3	2.01E3	24.38
	4	7.23E7	6.42E3	8.53E3	63.83
Test	2	3.75E7	3.91E3	2.06E3	24.66
	4	7.30E7	6.45E3	8.68E3	64.39

B.数据集V分类超分辨率性能

为了进一步评估SR数据的有效性，我们研究了使用SR数据对心理图像类进行分类的性能。深度神经网络(DNN)分类器被训练为HR和SR数据的预算特征使用预算特征类标签。DNN分类器由5个密集层组成，每层分别有512 256 128 64和3个神经元。所有层都包含ReLU[19]激活，不包括由Softmax激活组成的输出层。分类器采用ADAM优化器与learnig率的类交叉熵损失进行训练
 $-3 \quad 1=0.9$
 $2=0.99$ 。使用wgan的groundtruthHR数据和SR数据训练的Dnn的具有多个度量的类预测记录在表IV中。

表二。 DISCRIMINATOR MODEL ARCHITECTURE

层类型	Kernels	Dimensions	Activation
Convolution	64	(#输入通道+1 1)	Linear
Convolution	64	(1, 3)	ELU
Concatenate	-	-	-
Convolution	128	(#输入通道2+1 1)	ELU
Concatenate	-	-	-
Convolution	256	(#输入通道4+1 3)	ELU
Fully-Connected	128	-	ELU
Fully-Connected	1	-	Linear

IV.结果

A. Training & Hyperparameters

Dropout正则化[15]应用于生成器和鉴别器(不包括输出层)内的每个激活的输出。发生器和鉴别器的辍学率分别为0.1和0.25。将所有ELU[16]激活的全部elu[16]参数设为1。亚当优化器[17]在整个学习率中使用 $\alpha = 10^{-3}$ ， $\beta_1 = 0.9$ ， $\beta_2 = 0.99$ 。生成器网络首先使用mse(L2)损失进行预训练，用于50个epoch，小批量大小为64。所有超参数都进行了调整，以优化验证集的性能。

然后使用预训练的发电机进行微调。WGAN框架损失使用梯度惩罚权重为10。GAN训练比率被设置为3，每3个生成器更新一次鉴别器。除了WGAN损失函数之外，还对

表四。 CLASSIFICATION PERFORMANCE RESULTS

Scale	Metric (%)	Class	HR		WGAN	
			Val	Test	Val	Test
2	Precision	Precision	Accuracy	-	89.56	87.75
		Precision	Precision	2	89.70	86.65
		Precision	Precision	3	89.48	87.54
	Recall	Recall	Precision	7	89.57	88.77

V. DISCUSSION

On the topic of CNNs for EEG time-series data, we highlight below some of the important findings throughout our research. Feature scaling techniques besides standard normalization decreased model performance. With regards to convolutional layers, using kernel dimensions that contained weights for each channel in the input and output layers improved performance significantly over the standard kernel dimensions used for images, e.g., 3x3, 9x9. Implementing concatenation connections instead of residual connections, popular in ResNet [20] architectures used in many Super Resolution papers, offered improved performance using a lesser amount of layers. A Linear activation on the input layer followed by ELU activations on the subsequent layers outperformed other popular neural network activation functions combinations.

It was notably difficult and time-consuming to train GANs for EEG data. We observed after testing different variants of GAN that WGAN appeared to be more stable during training. Replacing MSE with MAE in all loss functions produced SR EEG signals which were smoothed and did not contain similar frequency domain statistics as the HR data. It can be concluded the task of EEG SR is highly sensitive to the loss function components used during training.

Observing the results in TABLE III. compared to bicubic interpolation, WGAN achieved $\sim 10^4$ fold and $\sim 10^2$ fold reduction in MSE and MAE, respectively, demonstrating the remarkable improvement of our proposed WGAN method in simultaneously reconstructing numerous missing EEG signals at a high resolution. Judging from the results in TABLE IV. it can be observed that classification of SR data produces minimal loss of accuracy when compared to ground truth signals, less than 4% and 9% for scale factors of 2 and 4, respectively.

VI. CONCLUSION

Our results conclude that our WGAN methods significantly improved over bicubic interpolation for the Dataset V EEG signals. We conclude that SR EEG by GAN is a promising approach to improve the spatial resolution of low density EEG headset. However we intend to expand our work to perform well across multiple datasets for different classification tasks. Considerations for further work also include using different distance metrics than MSE for assessing signal similarity as well as using other recent variations of the GAN framework to compare results.

ACKNOWLEDGMENT

This work was supported by the Army Research Laboratory Cognition and Neuroergonomics Collaborative Technology Alliance (CANCTA) under Cooperative Agreement Number W911NF-10-2-0022.

REFERENCES

- [1] J. Wolpaw and D. McFarland, "Multichannel EEG-based brain-computer communication," *Electroencephalography and Clinical Neurophysiology*, vol. 90, pp. 444-449, 1994.
- [2] L. Merino, T. Nayak, P. Kolar, G. Hall, Z. Mao, D. J. Pack, and Y. Huang, "Asynchronous control of unmanned aerial vehicles using a steady-state visual evoked potential-based brain computer interface," *Brain-Computer Interfaces*, vol. 4, pp. 122-135, 2017.
- [3] M. Hajinorozi, Z. Mao, T-P Jung, C-T Lin, and Y. Huang "EEG-based Prediction of Driver's Cognitive Performance by Deep Convolutional Neural Network," *Signal Processing: Image Communication*, vol. 47, pp. 549-555, 2016.
- [4] S. Petrichella et al., "Channel interpolation in TMS-EEG: A quantitative study towards an accurate topographical representation," *2016 38th Annual International Conference of the IEEE Engineering in Medicine and Biology Society (EMBC)*, pp. 989-992, 2016.
- [5] H. S. Courellis, J. R. Iversen, H. Poizner and G. Cauwenberghs, "EEG channel interpolation using ellipsoid geodesic length," *2016 IEEE Biomedical Circuits and Systems Conference (BioCAS)*, Shanghai, 2016, pp. 540-543. doi: 10.1109/BioCAS.2016.7833851
- [6] Y. Lecun, Y. Bengio, and G. Hinton, "Deep learning," *Nature*, vol. 521, pp. 436-444, 2015. doi: 10.1038/nature14539
- [7] C. Dong, K. He, C. Loy, and X. Tang, "Image Super-Resolution Using Deep Convolutional Networks," *IEEE Transactions on Pattern Analysis and Machine Intelligence*, vol. 38, pp. 295-307, 2016.
- [8] I. Goodfellow, J. Pouget-Abadie, M. Mirza, B. Xu, D. Warde-Farley, S. Ozair, A. Courville, and Y. Bengio, "Generative Adversarial Nets," *Advances in Neural Information Processing Systems*, vol. 27, pp. 2672-2680, 2014.
- [9] C. Ledig, L. Theis, F. Huszar, J. Caballero, A. Aitken, A. Tejani, J. Totz, Z. Wang, and W. Shi, "Photo-Realistic Single Image Super-Resolution Using a Generative Adversarial Network", 2016.
- [10] J. Millan, "On the need for on-line learning in brain-computer interfaces," *2004 IEEE International Joint Conference on Neural Networks (IEEE Cat. No.04CH37541)*, 2004, pp. 2877-2882 vol.4. doi: 10.1109/IJCNN.2004.1381116
- [11] M. Arjovsky, L. Bottou, and S. Chintala, "Wasserstein GAN," 2017.
- [12] F. Ahmed, M. Arjovsky, A. Courville, V. Dumoulin, and I. Gulrajani, "Improved Training of Wasserstein GANs," 2017.
- [13] W. Burgard, T. Ball, K. Eggensperger, L. Fiederer, M. Glasstetter, F. Hutter, R. Schirrmeyer, J. Springenberg, and M. Tangermann, "Deep learning with convolutional neural networks for EEG decoding and visualization," *Human brain mapping*, vol. 38, pp. 5391-5420y 2017.
- [14] G. Huang, Z. Liu, L. van der Maaten, and K. Weinberger, "Densely connected convolutional networks," in *Proceedings of the IEEE Conference on Computer Vision and Pattern Recognition*, 2017
- [15] N. Srivastava, G. Hinton, A. Krizhevsky, I. Sutskever, and R. Salakhutdinov, "Dropout: A Simple Way to Prevent Neural Networks from Overfitting," *Journal of Machine Learning Research*, vol. 15, pp. 1929-1958, 2014.
- [16] D. Clevert, T. Unterthiner, and S. Hochreiter, "Fast and Accurate Deep Network Learning by Exponential Linear Units (ELUs)," in *International Conference on Learning Representations*, 2016.
- [17] D. P. Kingma and J. Lei Ba, "ADAM: A Method for Stochastic Optimization," in *International Conference on Learning Representations*, 2015.
- [18] T. Salimans, I. Goodfellow, W. Zaremba, V. Cheung, A. Radford, X. Chen, "Improved Techniques for Training GANs," *Advances in Neural Information Processing Systems*, vol. 29, pp. 2234-2242, 2016.
- [19] G. Hinton, and V. Nair, "Rectified Linear Units Improve Restricted Boltzmann Machines," *International Conference on Machine Learning*, 2010
- [20] K. He, S. Ren, J. Sun, and X. Zhang, "Deep Residual Learning for Image Recognition," *IEEE Conference on Computer Vision and Pattern Recognition*, pp. 770-778, 2016

V. DISCUSSION

关于脑电图时间序列数据的CNNs主题，我们在下面强调了我们整个研究的一些重要发现。除标准归一化之外的特征缩放技术降低了模型性能。关于卷积层，在输入和输出层中使用包含每个通道权重的内核维度比用于图像的标准内核维度（例如3x3 9x9）显着提高了性能。实现串联连接而不是剩余连接，在许多ResNet[20]体系结构中很流行

使用较少的层提供了改进的性能。输入层上的线性激活，随后在随后的层上的ELU激活，优于其他流行的神经网络激活函数组合。

训练非常困难和耗时

用于脑电图数据。我们在测试GAN的不同变体后观察到，WGAN在训练期间似乎更稳定。在所有损失函数中用MAE替换MSE产生了sREEG信号，这些信号被平滑并且不包含与HR数据相似的频域统计信息。可以得出结论，脑电图SR的任务对训练过程中使用的损失函数分量高度敏感。

与双三次插值相比，WGAN在MSE和MAE中分别减少了~104倍和~102倍，这表明我们提出的WGAN方法在高分辨率下同时重建大量缺失的脑电信号方面有显着的改进。从表四的结果可以看出，与地面真相信号相比，SR数据的分类产生的准确性损失最小，2和4的比例因子分别低于4%和9%。

VI. CONCLUSION

与数据集V脑电信号的双三次插值相比WGAN方法得到了显着的改进。我们得出结论，GAN的SREEG是提高低密度EEG耳机空间分辨率的有希望的方法。但是，我们打算扩展我们的工作，以便在不同分类任务的多个数据集中表现良好。进一步工作的考虑还包括使用与MSE不同的距离度量来评估信号相似性以及使用GAN框架的其他最近变化来比较结果。

ACKNOWLEDGMENT

这项工作得到了陆军研究实验室的支持
Cognition and Neuroergonomics Collaborative Technology Alliance (CANCTA) under Cooperative Agreement Number W911NF-10-2-0022.

REFERENCES

- [1] J. Wolpaw and D. McFarland, "基于脑计算机通信的电脑电图和临床神经生理学", 卷.90, 第444-449页, 1994年。
- [2] L. Merino, T. Nayak, P. Kolar, G. Hall, Z. Mao, D. J. Pack, and Y. Huang, "使用稳态视觉诱发电位的无人机异步控制-脑机接口", 卷. 4, pp. 122-135 2017
- [3] M. Hajinorozi, Z. Mao, T-P Jung, C-T Lin, and Y. Huang "EEG中的信道插值：一个定量精确地形表示", "2016年第38届IEEE医学与生物学会国际年会 (EMBC)", 第989992页, 2016年
- [4] H. S. Courellis, J. R. Iversen, H. Poizner and G. Cauwenberghs, "EEG通道插值使用椭球测地线长度", "2016年IEEE生物医学电路和系统会议 (BioCAS)", 上海, 2016年, 第540-543页。doi: 10.1109/BioCAS.2016.7833851
- [5] Y. Lecun, Y. Bengio, and G. Hinton, "深度学习", 卷. 521, 第436-444页, 2015年。doi: 10.1038/nature14539
- [6] C. Dong, K. He, C. Loy, and X. Tang, "采用深度卷积网络的电子图像超分辨率", 《深度学习》, 卷. 521, 第436-444页, 2015年。doi: 10.1038.14539

分析与机器智能, 卷. 38, 第295-307页, 2016年。

[8] I. Goodfellow, J. Pouget-Abadie, M. Mirza, B. Xu, D. Warde-Farley, S. Ozair, A. Courville, and Y. Bengio, "生成式对抗网络", 《生成式对抗网络》，第267-2680页, 2014年。

[9] C. Ledig, L. Theis, F. Huszar, J. Caballero, A. Aitken, A. Tejani, J. Totz, Z. Wang, and W. Shi, "照片逼真的单图像超分辨率", 《深度学习》, 卷. 521, 第436-444页, 2015年。doi: 10.1038.14539

使用生成式对抗网络的分辨率率。[10] J. Millan "On the need for on-line learning in brain-computer interfaces" 2004 IEEE International Joint Conference on Neural Networks (IEEE Cat. No.04CH37541), 2004年, 第287-2882卷。doi: 10.1109/IJCNN.2004.1381116

[11] M. Arjovsky, L. Bottou, and S. Chintala, "Wasserstein GAN", 2017.

[12] F. Ahmed, M. Arjovsky, A. Courville, V. Dumoulin, and I. Gulrajani, "Improved Training of Wasserstein GANs", 2017.

[13] W. Burgard, T. Ball, K. Eggensperger, L. Fiederer, M. Glasstetter, F. Hutter, R. Schirrmeyer, J. Springenberg, and M. Tangermann, "Deep learning with convolutional neural networks for EEG decoding and visualization," Human brain mapping, vol. 38, pp. 5391-5420y 2017.

[14] G. Huang, Z. Liu, L. van der Maaten, and K. Weinberger, "Densely connected convolutional networks," in Proceedings of the IEEE Conference on Computer Vision and Pattern Recognition, 2017

[15] N. Srivastava, G. Hinton, A. Krizhevsky, I. Sutskever, and R. Salakhutdinov, "Dropout: A Simple Way to Prevent Neural Networks from Overfitting," Journal of Machine Learning Research, vol. 15, pp. 1929-1958, 2014.

[16] D. Clevert, T. Unterthiner, and S. Hochreiter, "Fast and Accurate Deep Network Learning by Exponential Linear Units (ELUs)," in International Conference on Learning Representations, 2016.

[17] D. P. Kingma and J. Lei Ba, "ADAM: A Method for Stochastic Optimization," in International Conference on Learning Representations, 2015.

[18] T. Salimans, I. Goodfellow, W. Zaremba, V. Cheung, A. Radford, X. Chen, "Improved Techniques for Training GANs," Advances in Neural Information Processing Systems, vol. 29, pp. 2234-2242, 2016.

[19] G. Hinton, and V. Nair, "Rectified Linear Units Improve Restricted Boltzmann Machines," International Conference on Machine Learning, 2010

[20] K. He, S. Ren, J. Sun, and X. Zhang, "Deep Residual Learning for Image Recognition," IEEE Conference on Computer Vision and Pattern Recognition, pp. 770-778, 2016

d为随机指标

在国际表示, 2015年。[18] T. Salimans, I. Goodfellow, W. Zaremba, V. Cheung, A. Radford, X. Chen, "神经信息处理系统中训练GANs的改进技术", 卷. 29, 第2234-2242页, 2016年。[19] G. Hinton, 和 V. Nair, "通过整流的线性单位改进", 《机器学习研究杂志》, 卷. 15, 第1929-1958页, 2014年。[20] D. Clevert, T. Unterthiner和S. Hochreiter通过指数线性单位 (ELUs) 实现快速准确的深度网络学习。[17]

来自Overfitting, 《机器学习研究杂志》, 卷. 15, 第1929-1958页, 2014年。[16] D. Clevert, T. Unterthiner和S. Hochreiter通过指数线性单位 (ELUs) 实现快速准确的深度网络学习。[17]

机器学习国际会议, 2010年[20] K. He, S. Ren, J. Sun和X. Zhang, "深度学习", 《深度学习》, 第770-778页 2016